

# Recent result from the A2 real photon facility at MAMI\*

Andreas Thomas<sup>1)</sup> (for the CBall@MAMI and A2 collaborations)

(Institut für Kernphysik, University Mainz, J.-J. Becherweg 45, D-55099 Mainz, Germany)

**Abstract** The upgraded MAMI C accelerator is delivering electrons with an energy of 1558 MeV routinely. The A2 collaboration is doing experiments with energy marked polarised real photons produced via “Bremsstrahlung”. Recent results from the GDH-experiment using a longitudinal polarised frozen spin target in combination with the DAPHNE detector and from the Crystal Ball experiment at MAMI are presented.

**Key words** photonuclear reactions, polarization phenomena in reactions, polarized and other targets, lepton-induced reactions

**PACS** 25.20.-x, 24.70.+s, 29.25.Pj

## 1 Introduction

Since more than 20 years the international A2 collaboration has been measuring photoabsorption cross sections of circularly polarized photons on unpolarised and longitudinally polarized protons to determine the total cross section and partial reaction channels in a large kinematical range, which provides new information about the excitation spectrum of the nucleon. The A2-Glasgow-Mainz tagging facility stands out due to its high photon intensity.

An extended experimental program to investigate the Gerasimov-Drell-Hearn (GDH) sum rule and related partial reaction cross sections on proton and neutron has been carried out by the GDH collaboration at the electron accelerators MAMI (Mainz) and ELSA (Bonn)<sup>[1–9]</sup>. In 2003 a new measurement with a highly polarised, deuterated butanol target has been performed in Mainz with the DAPHNE detector. Recently the high statistics data set has been published<sup>[10]</sup>.

In the years 2005/2006 the Crystal Ball detector with its unique capability to cope with multi photon final states was set up and used with polarized beams and unpolarized targets in Mainz. The experimental apparatus has been completed by polarized targets and a recoil polarimeter.

## 2 Photon beam

### 2.1 MAMI accelerator

The MAMI accelerator (Fig. 1) with its source of polarised electrons, based on the photoeffect on a strained GaAs crystal, routinely delivers polarised beams with a maximum energy of 1558 MeV. We typically have a degree of polarisation of about 85%. Details about the new machine type can be found in reference<sup>[11]</sup>.

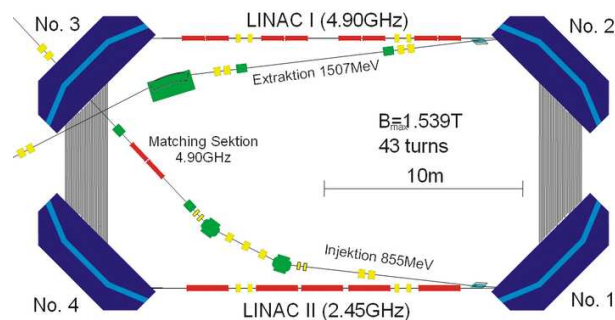


Fig. 1. The accelerator stage MAMI C is realized as a Harmonic Double Sided Microtron HDSM. Main features of this new machine concept are the four 90 bending magnets and the two LINACs working on 2.45 GHz and the first harmonic.

Received 7 August 2009

\* Supported by “DFG Sonderforschungsbereich” SFB 443 and European Community-Research Infrastructure Activity under FP6 Structuring the European Research Area Programme (Hadron Physics, contract number RII3-CT-2004-506078)

1) E-mail: thomas@kph.uni-mainz.de

©2009 Chinese Physical Society and the Institute of High Energy Physics of the Chinese Academy of Sciences and the Institute of Modern Physics of the Chinese Academy of Sciences and IOP Publishing Ltd

## 2.2 Glasgow tagger

The A2 photon beam is derived from the production of Bremsstrahlung photons during the passage of the MAMI electron beam through a thin radiator. The resulting photons can be circularly polarised, with the application of a polarised electron beam, or linearly polarised, in the case of a crystalline radiator. The degree of polarisation achieved is dependent on the energy of the incident photon beam ( $E_0$ ) and the energy range of interest, but currently peaks at  $\sim 75\%$  for linear polarisation (Fig. 3) and  $\sim 85\%$  for circular polarisation (Fig. 4). The maximum degree of linear polarisation should be further improved by 5 to 10% by the end of 2009 when the collimation and beam monitoring systems will be optimised for MAMI-C during the installation of the Frozen Spin Target. The Glasgow Photon Tagger (Fig. 2) provides energy tagging of the photons by detecting the post-radiating electrons and can determine the photon energy with a resolution of 2 to 4 MeV depending on the incident beam energy, with a single-counter time resolution  $\sigma_t = 0.117$  ns<sup>[12]</sup>. Each counter can operate reliably to a rate of  $\sim 1$  MHz, giving a photon flux of  $2.5 \times 10^5$  photons per MeV. Photons can be tagged in the momentum range from 4.7 to 93.0% of  $E_0$ .

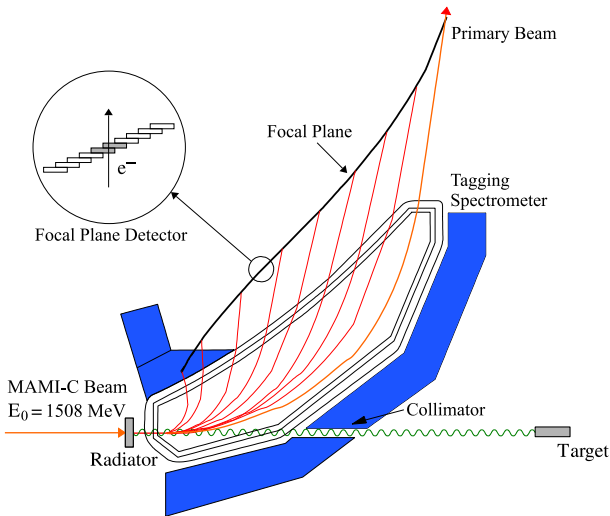


Fig. 2. The Glasgow photon tagging spectrometer.

To augment the standard focal plane detector system and make use of the Tagger's intrinsic energy resolution of 0.4 MeV (FWHM), there exists a scintillating fibre detector ("Tagger Microscope") that can improve the energy resolution by a factor of about 6 for a  $\sim 100$  MeV wide region of the focal plane (dependent on its position)<sup>[13]</sup>.

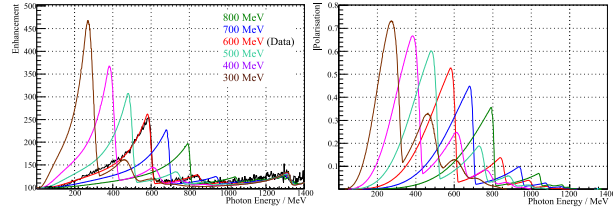


Fig. 3. Linear polarisation available with the current collimation system for a variety of crystal orientations. The thin black lines are data obtained during recent MAMI-C runs.

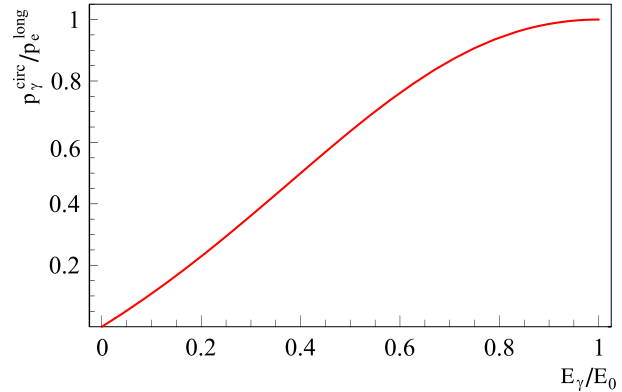


Fig. 4. Helicity transfer from the electron to the photon beam as function of the energy transfer. The MAMI beam polarisation is  $P_e \approx 85\%$ .

## 3 Detectors and recent results

### 3.1 GDH-apparatus and DAPHNE detector

A solid state "frozen spin" polarized target<sup>[14]</sup> from the Bonn polarised target group was used.

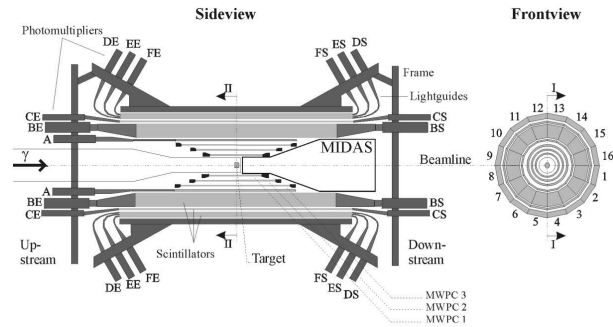


Fig. 5. The DAPHNE detector.

The cylindrical detector DAPHNE (Décteur a grande Acceptance pour la Physique photoNucléaire Experimentale)<sup>[15]</sup> was especially designed for handling multi particle final states by provision of a large solid angle (94% of  $4\pi$ ) particle identification and has a moderate efficiency for neutral particles. DAPHNE was developed by a collaboration of Saclay and Pavia for the investigation of photoreactions on light nuclei. As shown in Fig. 5, DAPHNE surrounds the

target and has a cylindrical symmetry. It consists of a vertex detector (three multi-wire proportional chambers, MWPC) for reconstructing the trajectories of charged particles surrounded by a hodoscope for their identification and energy determination. The outer part forms a lead-aluminum-scintillator sandwich serving as a calorimeter for the detection of decay photons and protons. Below a primary beam energy of 700 MeV all emitted protons are retained in the detector providing a good energy determination. The threshold momentum for the detection of charged particles emitted from a target including holding coil amounts to 80 MeV/c for pions and 270 MeV/c for protons. Leptonic background in DAPHNE is suppressed by the selection of appropriate discriminator thresholds. In forward direction further detection components (silicon  $\mu$ -strip detector, a Čerenkov detector, a scintillation counter array, the ring shaped STAR detector) have been added to expand the angular acceptance.

### 3.2 Recent results from the GDH-experiment

In 2003 a new measurement with a highly polarised, deuterated butanol target has been performed in Mainz with the DAPHNE detector. Recently the high statistics data set for the total inclusive polarised cross section difference on deuterium has been published<sup>[10]</sup>. In the upper part of Fig. 6 the helicity dependent total inclusive photoabsorption cross section obtained in this work (full circles) is compared

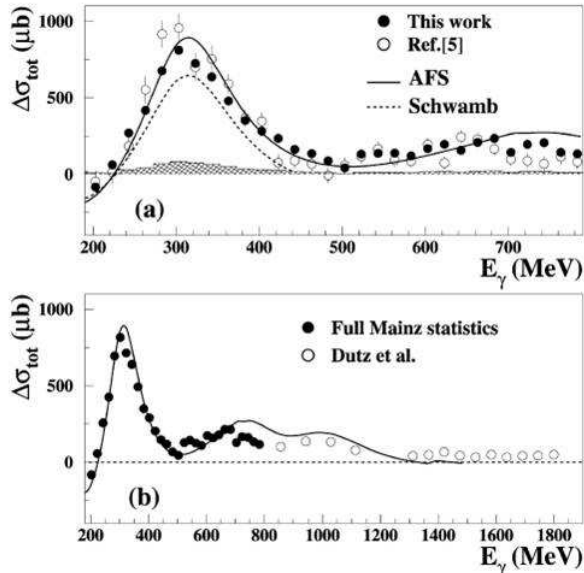


Fig. 6. (a) The helicity dependent total inclusive photoabsorption cross section; (b) The sum of all helicity dependent total inclusive data obtained at Mainz.

to previous results<sup>[9]</sup> (open circles) and to theoretical predictions of AFS<sup>[16]</sup> and Schwamb<sup>[17]</sup>. The hatched band shows the experimental systematic uncertainties. The statistical error bar has been improved significantly with this measurement. The lower part of Fig. 6 shows the sum of all helicity dependent total inclusive data obtained at Mainz (full circles), our previous results from Bonn<sup>[6]</sup> (open circles) for the higher energies and the predictions of the AFS<sup>[16]</sup> model.

In Fig. 7 the helicity dependent total cross section for the semi-exclusive channels  $\gamma d \rightarrow \pi^0 X$  ( $X = pn$  or  $d$ ) and  $\gamma d \rightarrow \pi^\pm NN$  (full circles) are compared to our previous results<sup>[9]</sup> (open circles) and to the corresponding model predictions in the  $\Delta$ -resonance region.

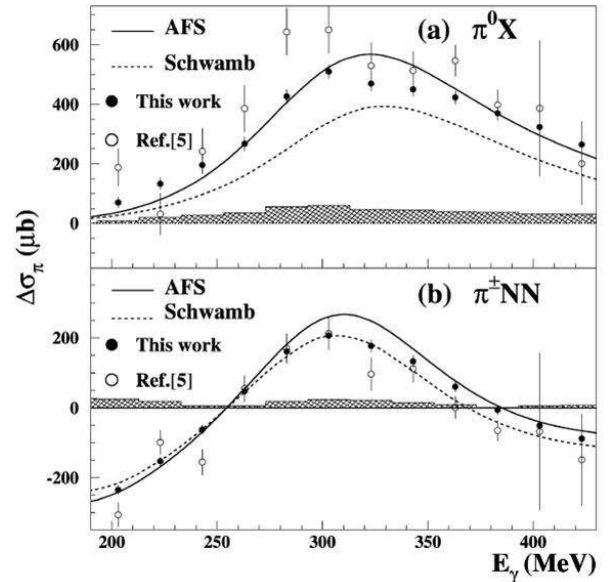


Fig. 7. The helicity dependent total cross section for the semi-exclusive channels.

## 4 Crystal Ball at MAMI

### 4.1 The new Frozen-Spin Target for Crystal Ball

Polarisation experiments using high density solid-state targets in combination with tagged photon beams can reach the highest luminosities. For the double polarisation measurements planned with the Crystal Ball detector on polarised protons and deuterons a specially designed, large horizontal  $^3\text{He}/^4\text{He}$  dilution refrigerator was built in cooperation with the Joint Institute for Nuclear Research (JINR) Dubna (see Figs. 8 and 9). It has minimum limitations for the particle detection and fits into the central core of the inner Particle Identification Detector

(PID2). This was achieved by using the frozen spin technique with the new concept of placing a thin superconducting holding coil inside the polarisation refrigerator. Longitudinal and transverse polarisations will be possible. In Fig. 10 the internal superconducting holding coils for transverse field operating at 1.2 K can be seen.



Fig. 8. The new dilution refrigerator for the Crystal Ball Frozen Spin Target.

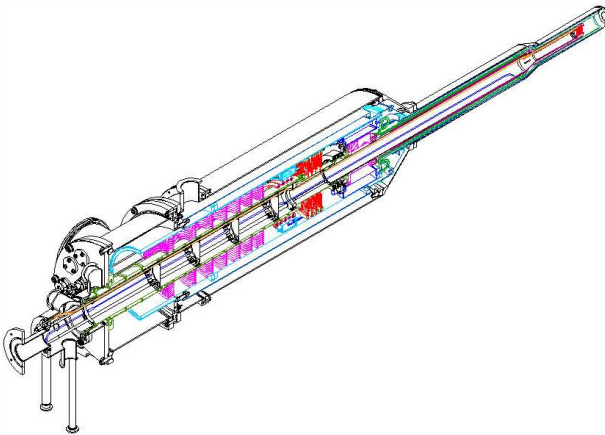


Fig. 9. Schematic view of the new dilution refrigerator.

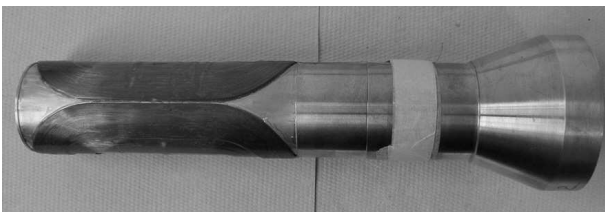


Fig. 10. The transverse holding coil.

Highest nucleon polarisation in solid-state target materials is obtained by a microwave pumping process, known as “Dynamic Nucleon Polarisation” (DNP). This process is applicable to any nucleus with spin and has already been used in different experiments with polarised proton and deuteron targets. The geometric configuration of the target is the same for the polarised proton and neutron setup. However, since the polarisation measurement of the deuteron is more delicate due to the small size of the polarisation signals, the modification of some basic components is needed. The reason for this is twofold: firstly the magnetic moment of the deuteron is smaller than that of the proton and, in addition, the interaction of the deuteron quadrupole moment with the electric field gradient in the sample broadens the deuteron polarisation signal. An accuracy  $\delta P_p/P_p$  of 2 to 3% for the protons and  $\delta P_D/P_D$  of 4 to 5% for the deuterons is expected in the polarisation measurement. It has also to be taken into account that the measured deuteron polarisation  $P_D$  is not equal to the neutron polarisation  $P_n$ . Assuming a 6% admixture of the D-state of the deuteron, a calculation based on the Clebsch-Gordon coefficients leads to  $P_n = 0.91 P_D$ . Several polarised proton and deuteron materials are available such as alcohols and deuterated alcohols (e.g. butanol  $C_4H_9OH$ ),  $NH_3$ ,  $ND_3$  or  ${}^6LiD$ . The most important criteria in the choice of material suitable for particle physics experiments are the degree of polarisation  $P$  and the ratio  $k$  of free polarisable nucleons to the total number of nucleons. Further requirements on polarised target materials are a short polarisation build-up time and a simple, reproducible target preparation. The polarisation resistance against radiation damage is not an issue for experiments with a low intensity tagged photon beam ( $\dot{N}_\gamma \approx 5 \times 10^7 s^{-1}$ ) as will be used here. However, the limitations of a reduced relaxation time due to overheating of the target beads (Kapitza resistance) will have to be investigated.

Taking all properties together, butanol and deuterated butanol are the best material for this experiment. For protons we expect a maximum polarisation of  $P_p = 90\%$  and an average polarisation of  $P_p = 70\%$  in the frozen spin mode. Recently, a deuteron polarisation  $P_D = 80\%$  was obtained with Trityl doped butanol targets at 2.5 T magnetic field in a  ${}^3He/{}^4He$  dilution refrigerator. At a 0.4 T holding field an average neutron polarisation  $P_n$  (see above) of 50% will be obtained. The filling factor for the  $\sim 2$  mm diameter butanol spheres into the 2 cm long, 2 cm diameter target container will be around 60%. The experience from the GDH runs in 1998<sup>[18]</sup> shows

that, with a total tagged photon flux of  $5 \times 10^7$ , relaxation times of about 200 hours can be expected. The polarisation has to be refreshed by microwave pumping every two days.

In conclusion, we estimate that we will achieve the following target parameters:

- 1) Maximum total tagged photon flux in the energy range of 4.7 to 93% of  $E_0$ :  $\dot{N}_\gamma \approx 5 \times 10^7 \text{ s}^{-1}$ , with relaxation time of 200 hours.
- 2) Target proton density in 2 cm cell:  $N_T \approx 9.1 \times 10^{22} \text{ cm}^{-2}$  (including dilution and filling factors)
- 3) Average proton polarisation  $P_p = 70\%$
- 4) Target deuteron density in 2 cm cell:  $N_T \approx 9.4 \times 10^{22} \text{ cm}^{-2}$  (including dilution and filling factors)
- 5) Average neutron polarisation  $P_n = 50\%$

#### 4.2 Crystal ball detector system

The central detector system consists of the Crystal Ball calorimeter combined with a barrel of scintillation counters for particle identification and two coaxial multiwire proportional counters for charged particle tracking. This central system provides position, energy and timing information for both charged and neutral particles in the region between  $21^\circ$  and  $159^\circ$  in the polar angle ( $\theta$ ) and over almost the full azimuthal ( $\phi$ ) range. At forward angles, less than  $21^\circ$ , reaction products are detected in the TAPS forward wall. The full, almost hermetic, detector system is shown schematically in Fig. 11 and the measured two-photon invariant mass spectrum is shown in Fig. 12.

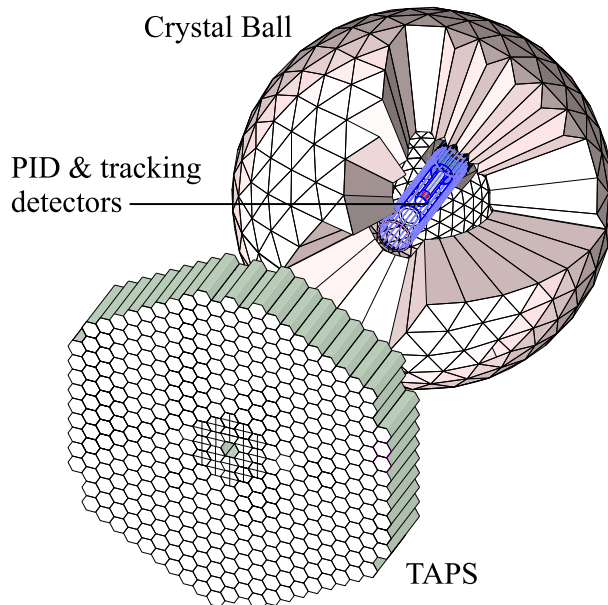


Fig. 11. The A2 detector setup: The Crystal Ball calorimeter, with cut-away section showing the inner detectors, and the TAPS forward wall.

The Crystal Ball detector (CB) is a highly segmented 672-element NaI(Tl), self triggering photon spectrometer constructed at SLAC in the 1970's. Each element is a truncated triangular pyramid, 41 cm (15.7 radiation lengths) long. The Crystal Ball has an energy resolution of  $\Delta E/E = 0.020E[\text{GeV}]^{0.36}$ , angular resolutions of  $\sigma_\theta = 2 \dots 3^\circ$  and  $\sigma_\phi = \sigma_\theta / \sin\theta$  for electromagnetic showers<sup>[19]</sup>. The readout electronics for the Crystal Ball were completely renewed in 2003, and it now is fully equipped with SADCs which allow for the full sampling of pulse-shape element by element. In normal operation, the onboard summing capacity of these ADCs is used to enable dynamic pedestal subtraction and the provision of pedestal, signal and tail values for each element event-by-event. Each CB element is also newly equipped with multi-hit CATCH TDCs. The readout of the CB is effected in such a way as to allow for flexible triggering algorithms. There is an analogue sum of all ADCs, allowing for a total energy trigger, and also an OR of groups of sixteen crystals to allow for a hit-multiplicity second-level trigger - ideal for use when searching for high multiplicity final states.

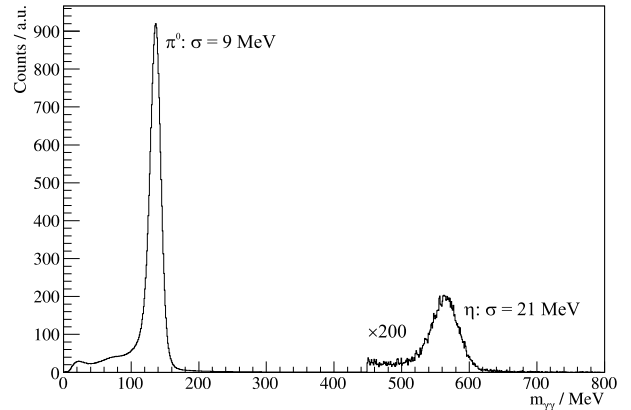


Fig. 12. Two photon invariant mass spectrum for the CB/TAPS detector setup. Both  $\eta$  and  $\pi^0$  mesons can be clearly seen.

In order to distinguish between neutral and charged particles species detected by the Crystal Ball, the system is equipped with PID2, a barrel detector of twenty-four 50 mm long, 4 mm thick scintillators, arranged so that each PID2 scintillator subtends an angle of  $15^\circ$  in  $\phi$ . By matching a hit in the PID2 with a corresponding hit in the CB, it is possible to use the locus of the  $\Delta E, E$  combination to identify the particle species (Fig. 13). This is primarily used for the separation of charged pions, electrons and protons. The PID2 covers from  $15^\circ$  to  $159^\circ$  in  $\theta$ .

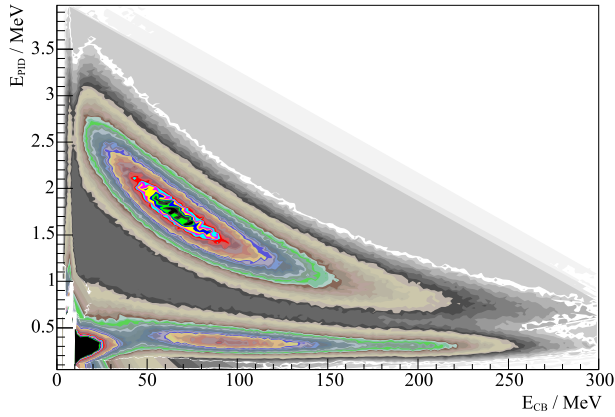


Fig. 13. A typical  $\Delta E/E$  plot from the Crystal Ball and the PID2 detector. The upper curved region is the proton locus, the lower region contains the pions and the peak towards the origin contains mostly electrons.

The excellent CB position resolution for photons stems from the fact that a given photon triggers several crystals and the energy-weighted mean of their positions locates the photon position to better than the crystal pitch. For charged particles which deposit their energy over only one or two crystals, this is not so precise. Here the tracks of charged particles emitted within the angular and momentum acceptance of the CB detector will be reconstructed from the coordinates of point of intersections of the tracks with two coaxial cylindrical multiwire proportional chambers (MWPCs) with cathode strip readout. These MWPCs are similar to those installed inside the CB during the first round of MAMI-B runs<sup>[20]</sup>. The most significant difference is that all detector signals are taken at the upstream end of the MWPCs, minimising the material required and facilitating particle detection in the forward polar region.

A mixture of argon (79.5%), ethane (30%) and freon-CF<sub>4</sub> (0.5%) is used as the filling gas. This mixture is a compromise between charge multiplication and localization requirements imposed by the ionizing particle tracks.

Within each chamber both the azimuthal and the longitudinal coordinates of the avalanche will be evaluated from the centroid of the charge distribution induced on the cathode strips. The location of the hit wires(s) will be used to resolve ambiguities which arise from the fact that each pair of inner and outer strip cross each other twice. The expected angular resolution (rms) will be  $\sim 2^\circ$  in the polar emission angle  $\theta$  and  $\sim 3^\circ$  in the azimuthal emission angle  $\phi$ .

The MWPCs have been recently installed inside the CB frame and their calibration using both cosmic rays and test beam data is currently underway.

### 4.3 TAPS forward wall

The TAPS forward wall is composed of 384 BaF<sub>2</sub> elements, each 25 cm in length (12 radiation lengths) and hexagonal in cross section, with a diameter of 59 mm. The front of every TAPS element is covered by a 5 mm thick plastic veto scintillator. The single counter time resolution is  $\sigma_t = 0.2$  ns, the energy resolution can be described by  $\Delta E/E = 0.018 + 0.008/E[\text{GeV}]^{0.5}$ <sup>[19]</sup>. The angular resolution in the polar angle is better than  $1^\circ$ , and in the azimuthal angle it improves with increasing  $\theta$ , being always better than  $1/R$  radian, where  $R$  is the distance in centimeters from the central point of the TAPS wall surface to the point on the surface where the particle trajectory meets the detector. The TAPS readout was custom built for the beginning of the CB@MAMI program and is effected in such a way as to allow particle identification by Pulse Shape Analysis (PSA), Time Of Flight (TOF) and  $\Delta E/E$  methods (using the energy deposit in the plastic scintillator to give  $\Delta E$ ). TAPS can also contribute to the CB multiplicity trigger and is currently divided into upto six sectors for this purpose. The 2 inner rings of 18 BaF<sub>2</sub> elements have been replaced recently by 72 PbWO<sub>4</sub> crystals each 20 cm in length (22 radiation lengths). The higher granularity improves the rate capability as well as the angular resolution. The crystals are operated at room temperature. The energy resolution for photons is similar to BaF<sub>2</sub> under these conditions<sup>[21]</sup>.

### 4.4 Recent results from Crystal Ball at MAMI

The Crystal Ball detector in combination with TAPS and the high intensity photon beam from A2 serves as an  $\eta$ -factory. More than 100 million  $\eta$ 's have been produced in the last years for the investigation of rare  $\eta$ -decays to look for C and CP-Violation and the  $\eta$ -Dalitz-decay. The huge data sample has been used to derive the Dalitz-Plot-Parameter  $\alpha$  in the  $\eta \rightarrow \pi^0 \pi^0 \pi^0$  decay. This parameter is sensitive to the quark-mass-differenz  $m_u - m_d$  between up- and down-quark. Results for this have been published for MAMI-B<sup>[22]</sup> and for MAMI-C<sup>[19]</sup>.

With the increased energy of 1558 MeV of MAMI-C we have now also the possibility to produce a high statistics  $\eta$ ' sample.

Another new paper on the "Search for the charge-conjugation-forbidden  $\omega \rightarrow \eta \pi^0$  decay" has been accepted for publication in PRC<sup>[23]</sup>.

A further goal of our measurements is to investigate the nucleons excitation spectrum. Our data set

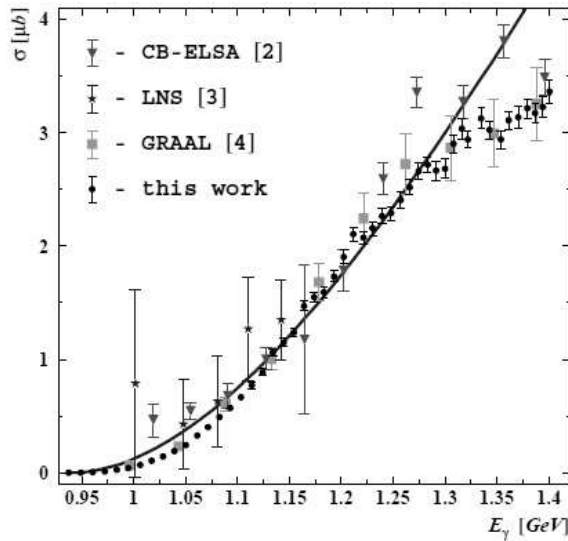


Fig. 14. Total cross sections for reaction  $\gamma p \rightarrow \eta\pi^0 p$ . The LNS and GRAAL points include both statistical and systematic uncertainties. For CB-ELSA and our points only statistical error bars are shown. The curve shows the energy dependence of the reaction phase space with arbitrary normalization.

with high statistics for pion and double pion production has been used to analyse the  $\eta\pi^0$ -production<sup>[24, 25]</sup>, for the quality of the measured total cross section see Fig. 14. The measured angular distributions are in qualitative agreement with the simplest calculation in which only the  $D_{33}$  partial-wave amplitude is included. This analysis confirms that in the energy region  $E < 1.4$  GeV the reaction  $\gamma p \rightarrow \eta\pi^0 p$  is dominated by the  $D_{33}$  partial wave which can naturally be associated with the resonance  $D_{33}(1700)$ . As background contributions are small,  $\eta\pi^0$ -photoproduction allows an almost background free study of the  $D_{33}(1700)$  baryon.

*The author wish to acknowledge the excellent support of the accelerator group and operators of MAMI, Schweizerischer Nationalfonds, the UK EPSRC and STFC, U.S. DOE, U.S. NSF, and NSERC (Canada). A.F. acknowledges additional support by the RF Presidential Grant (MD-2772.2007.2). We thank the undergraduate students of Mount Allison and George Washington Universities for their assistance.*

## References

- 1 Ahrens J et al. Phys. Rev. Lett., 2000, **84**: 5950
- 2 Ahrens J et al. Phys. Rev. Lett., 2002, **88**: 232002
- 3 Ahrens J et al. Phys. Lett. B, 2003, **551**: 49—55
- 4 Ahrens J et al. Eur. Phys. J. A, 2004, **21**: 323—333
- 5 Dutz H et al. Phys. Rev. Lett., 2004, **93**: 032003
- 6 Dutz H et al. Phys. Rev. Lett., 2005, **94**: 162001
- 7 Ahrens J et al. Phys. Lett. B, 2005, **624**: 173—180
- 8 Ahrens J et al. Phys. Rev. C, 2006, **74**: 045204
- 9 Ahrens J et al. Phys. Rev. Lett., 2006, **97**: 202303
- 10 Ahrens J et al. Phys. Rev. B, 2009, **672**: 328
- 11 Jankowiak A. EPJA, 2006, **28**(Suppl.1): 149—160
- 12 McGeorge J C et al. Eur. Phys. J. A, 2008, **37**: 129
- 13 Reiter A et al. Eur. Phys. J. A, 2006, **30**: 461
- 14 Bradtke C et al. Nucl. Instrum. Methods A, 1999, **436**: 430
- 15 Audit G et al. NIM A, 1991, **301**: 473
- 16 Arenhvel H, Fix A, Schwamb M. Phys. Rev. Lett., 2004, **93**: 202301
- 17 Schwamb M. Habilitation thesis, University of Mainz, 2006, Phys. Rep., in press
- 18 Thomas A et al. Nucl. Phys. B, 1999, **79**: 591
- 19 Prakhov S et al. Phys. Rev. C, 2009, **79**: 035204
- 20 Audit G et al. Nucl. Instrum. Methods A, 1991, **301**: 473
- 21 Novotny R et al. Nucl. Instrum. Methods A, 2002, **486**: 131
- 22 Unverzagt M et al. EPJ A, 2009, to be published
- 23 Starostin A et al. PRC, to be published
- 24 Kashevarov V et al. Photoproduction of  $\pi^0\eta$  on protons and the  $\Delta(1700)$   $D_{33}$  resonance, submitted to EPJ A and arXiv:0901.3888
- 25 Fix A, Ostrick M, Tiator L. Eur. Phys. J. A, 2008, **36**: 61—72